

## Determination of Kinetic Parameters for the Gasification of Biomass Char Using a Bubbling Fluidised Bed Reactor

Louise Lundberg<sup>1\*</sup>, Placid Atongka Tchoffor<sup>2</sup>, Robert Johansson<sup>1</sup>, David Pallarès<sup>1</sup>

<sup>1</sup>*Department of Energy and Environment, Chalmers University of Technology, SE-412 96 Göteborg, Sweden*

<sup>2</sup>*SP Technical Research Institute of Sweden, SE-501 15 Borås, Sweden*

*\*Telephone: +46 31 772 1438, E-mail: louise.lundberg@chalmers.se*

### Abstract

A laboratory scale bubbling fluidised bed is used to investigate the gasification kinetics of char from wood pellets. As expected, the experiments show that the char gasification rate increases with temperature, but also that it does not significantly depend on the steam concentration for the conditions investigated. The kinetic parameters are determined and three models accounting for changes in the char structure during char conversion are tested: the grain model, the random pore model and an empirical model. The empirical model is the only one which gives a satisfactory agreement with the experimental data obtained in the lab unit.

**Keywords:** Bubbling fluidised bed, biomass char gasification, kinetic parameters, modelling

### 1. Introduction

Thermogravimetric analysis (TGA) is often used to determine kinetic parameters for char gasification of biomass since very small particles can be studied, and thereby the influence of diffusion effects can be avoided. However, the reactivity of the char depends on the conditions under which the char is generated, such as the heating rate and whether or not the char is cooled between pyrolysis and char gasification [1]. In addition to this, crushing of the biomass to generate small particles affects the structure of the particles which could potentially influence the reactivity of the biomass. To ensure that the kinetic parameters determined are of quantitative relevance they should thus be obtained from experiments with full-size fuel particles and in conditions which mimic the conversion process in the larger unit of interest, in this case a fluidised bed. However, it is not obvious that the char conversion proceeds in the shrinking density regime in this type of experiments, since diffusion effects can be significant when large fuel particles are used. Also, the evolution of the internal surface area during the char conversion and the fragmentation of fuel particles are complex processes which can influence the char conversion rate. These processes are difficult to model and therefore result in additional uncertainties in this type of experiments. Although TGA still is the most commonly used technique to determine kinetic parameters for biomass char [1], there are some works that have considered char conversion in fluidised beds using larger particles. Nilsson et al. (2012) [2] investigated the char reactivity of dried sewage sludge using a fluidised bed reactor. They proposed an empirical structural model to describe the change of reactivity with the degree of conversion and concluded that it gave a satisfactory agreement with their experimental data. This model will, together with two other structural models, be tested in the present work.

The aim of this work is to investigate char gasification of wood pellets in fluidised beds and to describe the char conversion with a combination of kinetic parameters and a model for how the reactivity is affected by the degree of char conversion.

### 2. Theory

The degree of char conversion,  $X$ , is defined as:

$$X(t) = \frac{m_0 - m(t)}{m_0} \quad (1)$$

Two definitions of the reactivity are used in this work: the conversion rate,  $R_m$ , which is normalised with the initial mass of the char particle (Eq. 2) and the instantaneous rate,  $R_i$ , which is normalised using the mass of char at a given time (Eq. 3).  $R_i$  is used to qualitatively compare how the reactivity changes with conversion for different experiments while  $R_m$  is used in the modelling of the char reactivity.

$$R_m = \frac{dX(t)}{dt} = -\frac{1}{m_0} \frac{dm(t)}{dt} \quad (2)$$

$$R_i = -\frac{1}{m(t)} \frac{dm(t)}{dt} = -\frac{1}{m_0(1-X(t))} \frac{dm(t)}{dt} = R_m \cdot \frac{1}{(1-X(t))} \quad (3)$$

The rate of char gasification,  $R_m$ , can be expressed as [3]:

$$R_m = R(T, P_{H_2O})f(X) \quad (4)$$

Assuming  $n^{\text{th}}$  order kinetics, the dependence of the reactivity on temperature and steam pressure is given by:

$$R(T, P_{H_2O}) = k_0 e^{\frac{-E_a}{RT}} P_{H_2O}^n \quad (5)$$

In Eq. 4,  $f(X)$  describes how changes in the char structure during the conversion process influence the char reactivity. Of the different models proposed to describe this effect, two are commonly used: the grain model [4] and the random pore model [5]. Nilsson et al. (2012) [2] studied gasification of char from sewage sludge with  $H_2O$  or  $CO_2$  in a fluidised bed using particle sizes between 1.2 mm and 4.5 mm, i.e. conditions similar to those in this work. They found that none of the models proposed in the literature gave a satisfactory fit with their experimental results and suggested an empirical model on the following form:

$$f(X) = (1-X)(aX+b)\exp(-cX^d) \quad (6)$$

The three models for  $f(X)$  examined in this work are summarised in Table 1.

**Table 1. Models used to describe how the conversion rate depends on the degree of conversion.**

Model	f(X)	Parameters
Grain model (GM)	$(1-X)^{2/3}$	-
Random pore model (RPM)	$(1-X)\sqrt{1-\Psi\ln(1-X)}$	$\Psi$
Empirical model (EM)	$(1-X)(aX+b)\exp(-cX^d)$	a, b, c, d

### 3. Experiments

A schematic of the experimental setup is shown in Fig. 1. The inner diameter of the reactor is 7 cm and its total height is 140 cm. Distilled water (1) is transported at a controlled rate by a water pump (2) to a steam generator (3). The flow rate of nitrogen (or air during combustion) is set using a mass flow regulator (4) and the gases are preheated in the 60 cm high preheating zone (5) before entering the reactor through a perforated ceramic plate made of a hastelloy-X alloy consisting of pores with a diameter of 10  $\mu\text{m}$  (6), above which the fluidised bed (7) is located. 400 g of silica sand is used as bed material, which generates a bed height of approximately 4 cm. The reactor is electrically heated by heating elements (8) on the reactor walls. A K-type thermocouple inserted into the bed of the reactor is used to measure the bed temperature, which is controlled by a temperature regulator connected to the heating elements on the reactor walls. Fuel particles are inserted at the top of the reactor (9). A gas probe (10) is used to sample a slip stream while the rest of the gases generated enter the exhaust hood (11). The sampled gases are transferred through a particle filter (12) with the aid of a gas pump (13). The gases then pass through a condenser where the steam and tars are

condensed (14) before reaching the gas analysers (15) which measure the concentrations of CO, CO<sub>2</sub> and O<sub>2</sub>. Two types of gas analysers were used to measure the concentrations of CO and CO<sub>2</sub>, one high-range (CO<sub>2</sub>: 0-20% ± 0.47 pp, CO: 0-30,000 ppm ± 714.92 ppm) and one low-range with a higher accuracy (CO<sub>2</sub>: 0-5% ± 0.27 pp, CO: 0-20,000 ppm ± 296.06 ppm). Finally the output from the gas analysers is transformed using a pc logger (16) and the data is logged on a computer (17) every fifth second.

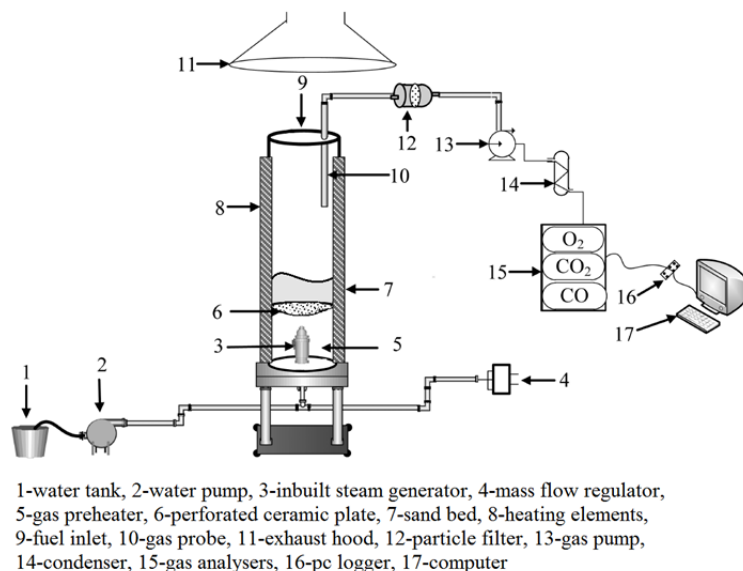


**Figure 1. Experimental setup.**

Pure N<sub>2</sub> was first used as the fluidising gas to allow pyrolysis of the wood pellets which were dropped into the pre-heated reactor. After ensuring complete pyrolysis - approximately three minutes - the gas flow into the reactor was switched to a mixture of steam and nitrogen (see Table 2) to allow char gasification. After a given retention time (15-25 minutes, see Table 2) the experiment was terminated and air was used to combust any remaining char, while still monitoring the CO and CO<sub>2</sub> concentrations to allow closure of the carbon balance (Table 2). In two cases (Experiments 1 and 7) it was not possible to calculate the carbon balance due to overheating of the O<sub>2</sub> analyser at the end of the experiments. The carbon balance was calculated by dividing the total measured mass of carbon from the char gasification and combustion with the initial mass of carbon,  $m_0$ . Elutriation of char fines was thus not included in the balance. However, since char fines have a lower resistance to steam mass transfer than large char particles they are likely to be converted rather fast, so it is plausible that most of the fines were converted in the reactor. The particle filter (12 in Fig. 1) mainly contained condensed tar after the experiments.

Nine experiments were conducted at different temperatures (758-875°C) and steam concentrations (58-89%<sub>vol</sub>), see Table 2. For experiments 1-8 the weight of the fuel particles was close to 10 g whereas it was somewhat lower (8.5 g) for experiment 9. Ten pellets were used in each experiment, each with a diameter of 8 mm and with lengths ranging between 13 and 20 mm. The fluidisation velocity during pyrolysis was 0.25-0.27 m/s whereas it was somewhat higher during char gasification (0.33-0.37 m/s).

**Table 2. Experimental matrix.**

Experiment	Temperature [°C]	Steam concentration [% <sub>vol</sub> ]	Mass of fuel [g]	Char gasification test time [min]	Accuracy in carbon balance [%]
1	856	89	9.974	20	-
2	854	69	9.940	24	98.0
3	855	58	9.992	15	100.1

4	758	89	9.970	22	100.9
5	774	89	9.973	22	97.0
6	802	89	9.978	22	101.4
7	819	89	10.058	20	-
8	875	89	9.976	20	96.4
9	840	72	8.506	25	102.1

## 4. Results and Discussion

### 4.1. Experimental results

Time-averaged char conversion rates for the first 15 minutes of the nine experiments are presented in Fig. 2. The reactivity increases with temperature as expected. However, the steam concentration does not significantly affect the reactivity; at 855 °C the reactivity is essentially the same for the three steam concentrations investigated.

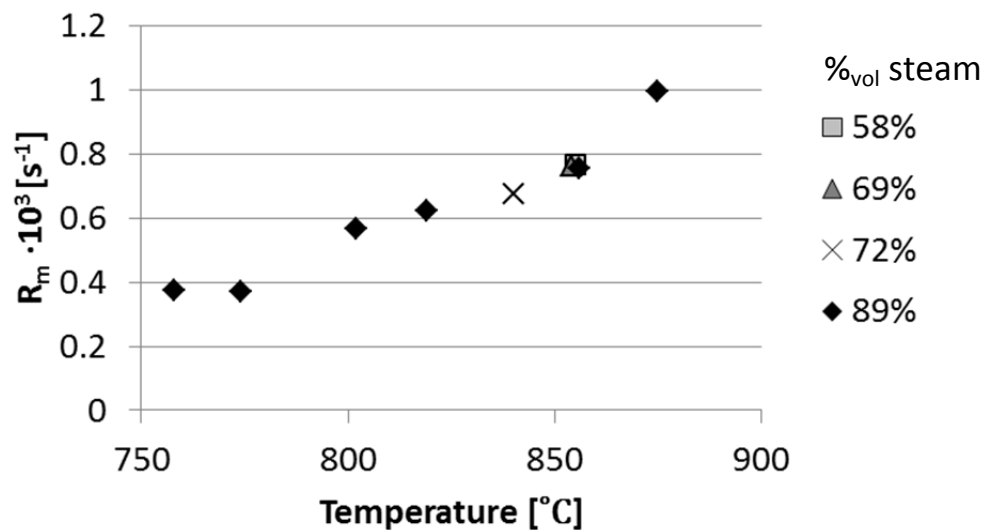


**Figure 2. Time-averaged char gasification rates,  $R_m$ , during the first 15 minutes of all the experiments.**

The instantaneous char conversion rate as a function of the degree of char conversion for experiments 1-3 is presented in Fig. 3. Between  $X = 0.2$  and  $X = 0.6$  the rate is very similar for all three steam concentrations. One explanation to this could be that the activated surface area of the char is fully occupied at  $X > 0.2$  for a steam concentration of 58%. If the steam concentration is increased, this would not significantly increase the reaction rate since there are no more active sites available. This explanation is supported by the work by Sun and Jiang (2010) [6], who used steam at different flow rates to activate char particles. They observed very small differences in activated surface area between samples subjected to a steam flow rate of 6 kg/h and 8 kg/h, indicating that no additional activation took place as the steam flow rate was increased.

Initially, however, the conversion rate is higher at higher steam concentrations. The reaction rate could be controlled by diffusion during this first part of the char conversion ( $X < 0.2$ ), as the particles are relatively large at this stage, giving a reaction rate that increases with concentration. However, at  $X > 0.2$  the diffusion resistance no longer seems to be the dominating factor. One explanation to this could be particle fragmentation: as the particles decrease in size, the resistance to external diffusion also decreases. In Fig. 4, which shows a photo of pellets which have been removed from the reactor using a basket arrangement after 25 minutes of char gasification, secondary fragmentation of the char particles can be observed. It should be noted that the fluctuations which can be observed in Fig. 3 are quite large, especially for experiment 1. Thus, there is some uncertainty in the differences in reactivity observed for the different steam concentrations during the conversion process.

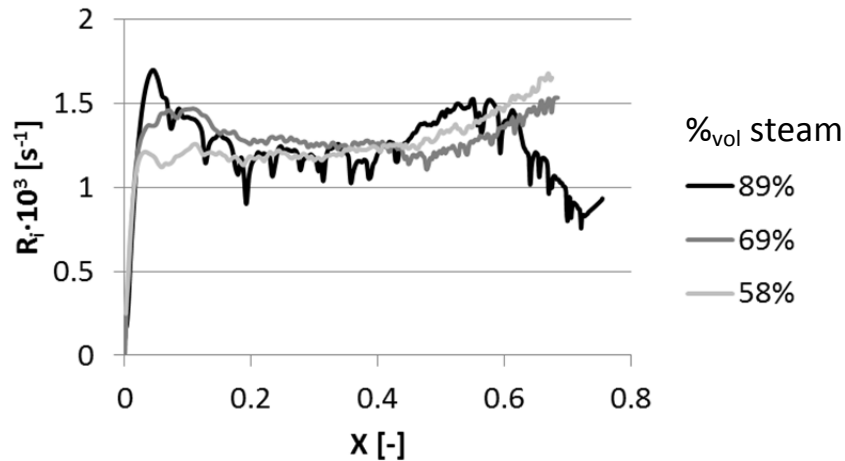


**Figure 3. Instantaneous rate as a function of the degree of conversion for three different steam concentrations at 855°C (experiments 1-3).**



**Figure 4. Pellets extracted after 25 minutes of char gasification at 840°C and a steam concentration of 72% (same conditions as for experiment 9).**

Figure 5 shows how the instantaneous char conversion rate changes with the degree of char conversion for three different temperatures. The same type of behaviour is seen for all curves in Figs 3 and 5 (except for the final part of experiment 1); initially the conversion increases sharply, reaches a maximum and then starts to decrease again before stabilising for a while. At the end of conversion it begins to increase again. This behaviour could be caused by the evolution of the activated internal surface area of the particles. According to Tchoffor et al. (2014) [7], the activated internal surface area is rather low after pyrolysis but when the char particles come into contact with steam the surface area becomes activated, leading to an increase in the reactivity. (However, it should be noted that there is some uncertainty in the measurements during the initial part of the conversion, since mixing and diffusional effects caused by the transportation of gases from the reactor to the measurement devices result in a delay of the measured concentrations.) After the initial stage, the amount of activated surface area peaks and starts to reduce as the conversion progresses, leading to a decrease in the reactivity.

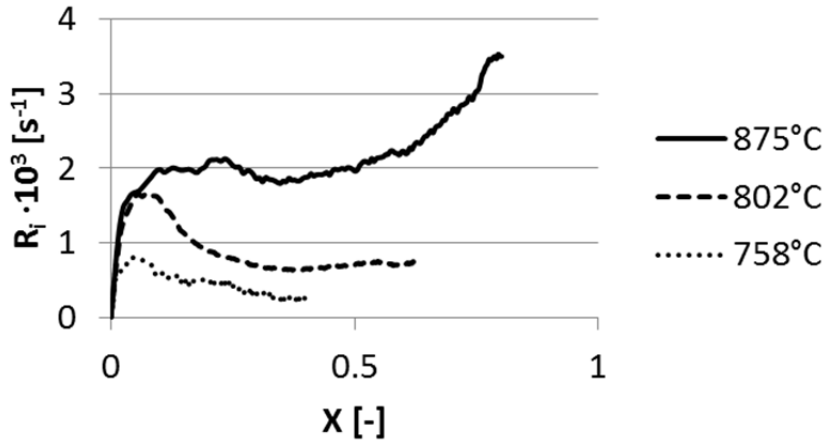


**Figure 5. Instantaneous reaction rate as a function of the degree of char conversion for three different temperatures and a steam concentration of 89% (experiments 4, 6 and 8).**

In addition to the reduction of the activated surface area described above, the influence of the permeability of the active sites on reactivity could explain the relatively fast decrease in the reactivity observed at 802°C. Shabanzadeh (2012) [8] activated char from wood pellets pyrolysis and studied their porosity with scanning electron microscopy (SEM). While the pore walls of the char samples activated at 900°C were firm, those in the char samples activated at 800°C collapsed against each other. If the pore walls collapse against each other, the active sites in the char matrix will be less permeable to steam and this would lead to an increase in the resistance to internal mass transfer. The referred finding may explain the discrepancy in the reactivities observed at 802°C and 875°C in the present work.

The observed peaks in reactivity are probably also partly due to the gasification of the small amount of char fines generated during pyrolysis. The fines are very small, thus they will only experience a small resistance to diffusion, and their reactivity might be higher than that of the larger char particles formed during pyrolysis. Li et al. (2014) [9], who compared the CO<sub>2</sub> gasification of coal char particles and fine char, found that the reactivity of the fines was higher than that of the larger char particles, owing to the larger surface area of the fines.

The rapid increase towards the end of the conversion which is especially prominent at 875°C is likely due to increased attrition in the light char structures and a collapse of the internal structure of the particles as the particles fragment followed by an increase in the available surface area.

#### 4.2. Kinetic modelling

The intrinsic kinetic parameters should be determined from data in the kinetic regime (i.e. a regime without significant diffusion effects). As discussed above, Fig. 3 shows that the instantaneous rate is very similar for all three steam concentrations considered for  $X > 0.2$ , and a possible explanation is that the activated sites of the char are fully occupied for all three cases. There is accordingly a surplus of water vapour that cannot react and is allowed to diffuse into the particles, which imply that there are no diffusion limitations. This indicates that the conversion is controlled by the kinetics in the later parts of the experiments. Also the fragmentation of the particles observed in the experiments reduces the diffusion resistances. The work presented below is based on the assumption that a kinetically controlled regime has been reached at a degree of conversion of 30% for all the experiments in this work. Nilsson et al. (2012) [2] also used a reference reactivity at 30% conversion, and could see that the conversion of their particles, up to 3.4 mm in size, was controlled by kinetics at a temperature of 850°C. However, further investigations are needed to fully assure that the conditions examined in this work are characterised by kinetic control.

Figure 6 shows an Arrhenius plot of the conversion rate at  $X = 30\%$  for those cases operating at a steam concentration of 89%. The pre-exponential factor and the activation energy obtained from this plot are presented in Table 3.

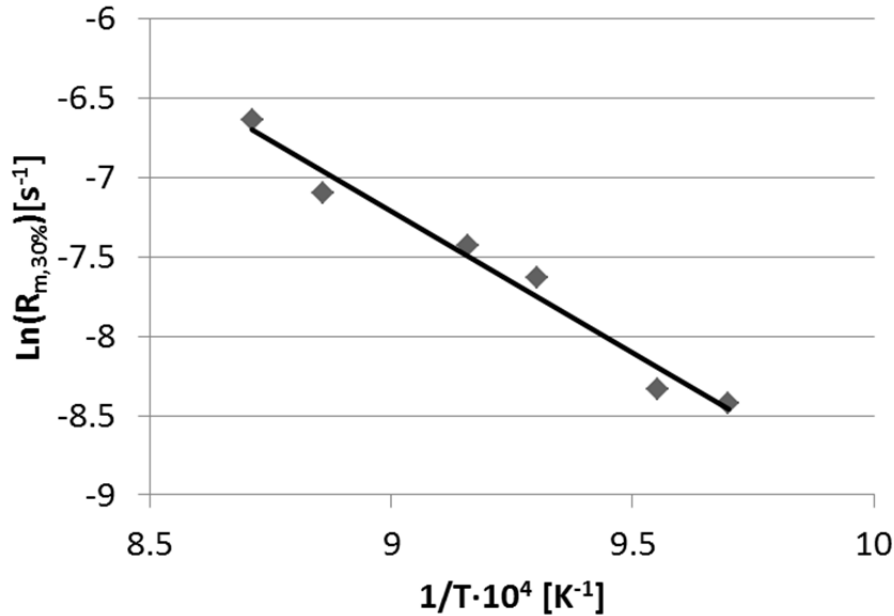


**Figure 6. Arrhenius plot for the conversion rate at X = 30% at a steam concentration of 89%.**

As discussed above, the dependency of the steam concentration on the rate of conversion is small for the range of concentrations studied. It is thus impossible to determine a value for  $n$  in Eq. 5. According to a review by Di Blasi (2009) [10],  $n$  usually lies between 0.4 and 1 for steam gasification of biomass, although other authors have reported lower values (e.g. Nilsson et al. (2012) [2] who found that  $n = 0.33$ ). The fact that no dependency on the steam concentration could be observed at the high steam concentrations studied in this work indicates that  $n$  should be rather low, since this leads to a small change in  $R$  in Eq. 5 when  $P_{H_2O}$  is varied at high concentrations. It was thus set to the lowest value proposed by Di Blasi (2009) [10], 0.4 (Table 3), but more experiments at lower steam concentrations should be carried out to be able to find a more reliable value for  $n$ . It should be noted that the choice of  $n$  affects the value of the pre-exponential factor,  $k_0$ .

**Table 3. Kinetic parameters and order of reaction obtained for the char gasification. Experimental ranges tested: temperature (758-875°C), steam concentration (58-89%).**

$k_0$ [bar <sup>-0.1</sup> s <sup>-1</sup> ]	$E_a$ [kJ/mol/K]	$n$ [-]
7234.5	148.3	0.4

Finally, the dependence of the reactivity on the degree of char conversion has to be determined. To be able to do this, most of the conversion process needs to be considered. Three of the experiments conducted at lower temperatures (5-7) were chosen for the parameter fit, since they are more likely to be in the kinetic regime. The constants obtained from the parameter fit for the random pore model and the empirical model are shown in Table 4.

**Table 4. Fitted parameters for the random pore model and the empirical model.**

$\Psi$ [-]	$a$ [-]	$b$ [-]	$c$ [-]	$d$ [-]
3.602	$2.096 \cdot 10^5$	$1.817 \cdot 10^5$	12.63	0.05064

Since none of the structural models in Table 1 are able to reproduce the sharp increase in reactivity in the initial part of char conversion (see Fig.7), a phase during which the activation of the internal surface area takes place, the fitting of the parameters in Table 1 was made from X = 5% (the peak in conversion takes place at a conversion of approximately 5% for all the experiments) to the end of the experiments. (As mentioned above, the accuracy of the measurements in the initial part of the

conversion is rather low due to diffusion and mixing effects during the transportation of the gases to the measurement devices.) A validation of the models is given in Fig. 7, which shows a comparison of the experimental and modelled char reactivity for experiment 4 (not used for the fitting). Since the reaction rates for the different models were calculated using the experimental temperature, which varied slightly during the course of the experiment, there are small fluctuations in the modelled reactivities in Fig. 7.

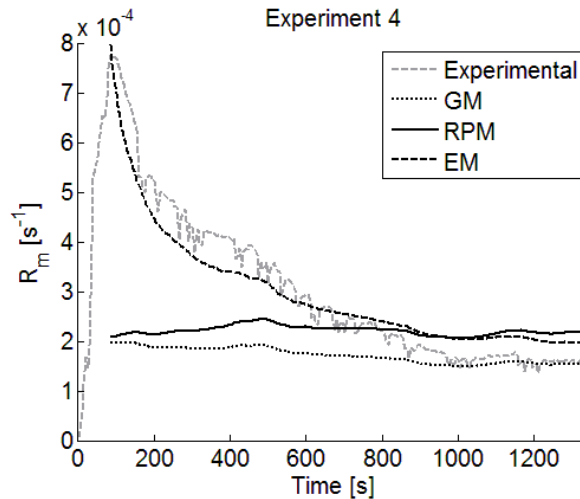


**Figure 7. Experimental and modelled conversion rates as a function of time for experiment 4 comparing the three different structural models  $f(X)$ .**

As can be seen in Fig. 7, only the empirical model gives a curve which resembles the experimental conversion rate for experiment 4. It should be emphasised that experiment 4 was not included in the parameter fit, and still the empirical model gives a good agreement with the experiment. The significant influence of the degree of conversion on the reactivity also stresses the need of studying these phenomena in conditions of practical relevance.

## 5. Conclusions

The char gasification reactivity of wood pellets has been investigated in a fluidised bed reactor. The char gasification rate increases with temperature but does not significantly depend on the steam concentration within the operational intervals studied (temperature: 758-875°C, steam concentration: 58-89%<sub>vol</sub>).

The kinetic parameters were determined, and an empirical structural model for the evolution of the char structure was shown to give a satisfactory description of the influence of conversion on the reactivity.

## Notation

### Roman letters

$a$	parameter used in the EM [-]
$b$	parameter used in the EM [-]
$c$	parameter used in the EM [-]
$d$	parameter used in the EM [-]
$f(X)$	structural model [-]
$E_a$	activation energy [kJ/mole]
$k_0$	pre-exponential factor [ $\text{bar}^{-0.1}\text{s}^{-1}$ ]
$m$	mass of carbon [kg]
$m_0$	initial mass of carbon [kg]
$n$	exponent of the gaseous reactant (steam) [-]

$P_{H_2O}$	steam pressure [bar]
$R$	reaction rate [ $\text{s}^{-1}$ ]
$R$	gas constant [J/mole/K]
$R_i$	instantaneous reaction rate [ $\text{s}^{-1}$ ]
$R_m$	conversion rate [ $\text{s}^{-1}$ ]
$t$	time [s]
$T$	temperature [K]
$X$	degree of conversion [-]

### Greek letters

$\Psi$	parameter used in the RPM [-]
--------	-------------------------------



## References

- [1] Gómez-Barea A, Leckner B, *Modeling of biomass gasification in fluidized bed*, Prog Energy Combust Sci 36 (2010) p. 444–509.
- [2] Nilsson S, Gómez-Barea A, Fuentes-Cano D, *Gasification reactivity of char from dried sewage sludge in a fluidized bed*, Fuel 92 (2012) p. 346-353.
- [3] Lu GQ, Do DD, *Comparison of structural models for high-ash char gasification*, Carbon 32 (1994) p. 247-263.
- [4] Ishida M, Wen CY, *Comparison of zone-reaction model and unreacted-core shrinking model in solid-gas reactions – I Isothermal analysis*, Chem Eng Sci 26 (1971) p. 1031-1041.
- [5] Bhatia SK, Perlmutter DD. *A random pore model for fluid-solid reactions: I. Isothermal, kinetic control*, AIChE Journal 26 (1980) p. 379–86.
- [6] Sun K, Jiang J, *Preparation and characterization of activated carbon from rubber-seed shell by physical activation with steam*, Biomass Bioenerg 34 (2010) p. 539-544.
- [7] Tchoffor PA, Davidsson K, Thunman H, *Effects of Steam on the Release of Potassium, Chlorine, and Sulfur during Char Conversion, Investigated under Dual-Fluidized-Bed Gasification Conditions*, Energ Fuel 28 (2014) p. 6953–6965.
- [8] Shabanzadeh A, *Production of activated carbon within the indirect gasification process*, Master's thesis at the Institution for Energy and Environment, Division for Energy Technology, Chalmers University of Technology, Göteborg, Sweden, 2012.
- [9] Li F, Li Z, Huang J, Fang Y, *Characteristics of fine chars from fluidized bed gasification of Shenmu coal*, J Fuel Chem Technol 42 (2014) p. 1153-1159.
- [10] Di Blasi C, *Combustion and gasification rates of lignocellulosic chars*, Prog Energy Combust Sci 35 (2009) p. 121-140.